Water adsorption on free cobalt cluster cations

Kiawi, D.M.; Bakker, J.M.; Oomens, J.; Buma, W.J.; Jamshidi, Z.; Visscher, L.; Waters, L.B.F.M.

DOI
10.1021/acs.jpca.5b07119

Publication date
2015

Document Version
Final published version

Published in
The Journal of Physical Chemistry. A

THE JOURNAL OF PHYSICAL CHEMISTRY A

Article

pubs.acs.org/JPCA

Water Adsorption on Free Cobalt Cluster Cations

Denis M. Kiawi,[†] Joost M. Bakker,[*,†] Jos Oomens,[†] Wybren Jan Buma,[‡] Zahra Jamshidi,[∥] Lucas Visscher,[⊥] and L. B. F. M. Waters[§,#]

[†]Radboud University, Institute for Molecules and Materials, FELIX Laboratory, Toernooiveld 7, 6525 ED Nijmegen, The Netherlands

[‡]Van't Hoff Institute for Molecular Sciences and [§]Anton Pannekoek Institute, University of Amsterdam, Science Park 904, 1098 XH Amsterdam, The Netherlands

[∥]Department of Physical Chemistry, Chemistry and Chemical Engineering Research Center of Iran, P.O. Box 14335-186, Tehran, Iran

[⊥]Amsterdam Center for Multiscale Modeling Section Theoretical Chemistry, VU University Amsterdam, De Boelelaan 1083, 1081 HV Amsterdam, The Netherlands

[#]SRON Netherlands, Sorbonnelaan, Utrecht, The Netherlands

ABSTRACT: Cationic cobalt clusters complexed with water Co_n^+–H_2O (n = 6–20) are produced through laser ablation and investigated via infrared multiple photon dissociation (IR-MPD) spectroscopy in the 200–1700 cm^{-1} spectral range. All spectra exhibit a resonance close to the 1595 cm^{-1} frequency of the free water bending vibration, indicating that the water molecule remains intact upon adsorption. For n = 6, the frequency of this band is blue-shifted, but it gradually converges to the free water value with increasing cluster size. In the lower-frequency range (200–650 cm^{-1}) the spectra contain several bands which show a very regular frequency evolution, suggesting that the exact cluster geometry has little effect on the water–surface interaction. Density functional theory (DFT) calculations are carried out at the OPBE/TZP level for three representative sizes (n = 6, 9, 13) and indicate that the vibrations responsible for the resonances correspond to bending and torsional modes between the cluster and water moieties. The potential energy surfaces describing these interactions are very shallow, making the calculated harmonic frequencies and IR intensities very sensitive to small geometrical perturbations. We conclude that harmonic frequency calculations on (local) minima structures provide insufficient information for these types of cluster complexes and need to be complemented with calculations that provide a more extensive sampling of the potential energy surface.

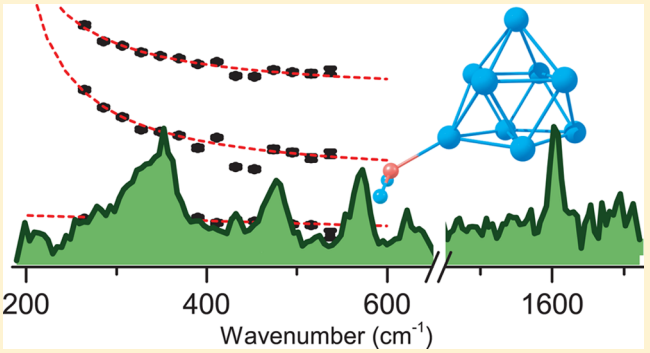

INTRODUCTION

Water is one of the most important chemicals on our planet, playing a role in virtually all aspects of life. Its interaction with metal surfaces is of fundamental importance, in particular, for electrochemical and catalytic processes.[1−4] On the molecular level, the study of this interaction translates into seemingly simple questions: what are the binding sites, the binding energy, and the structure of the adsorbed water?

On bulk metal surfaces, water tends to bind in an erect configuration with the oxygen atom pointing toward the surface while the hydrogen atoms are oriented away from it. Intuitively, one would expect the plane of the water dipole to be oriented perpendicular to the surface. However, theoretical studies suggest an alternative binding motif where the water is bound in an atop adsorption site with the O–H bonds directed nearly parallel to the surface.[5] Experimental information can be obtained from the combination of various experimental techniques, such as low-energy electron diffraction (LEED), scanning-tunneling microscopy (STM),[6] or reflection–absorption IR spectroscopy (RAIRS). The number of studies on the interaction of water with cobalt surfaces, while of fundamental interest for important industrial processes such as the Fischer–Tropsch synthesis, has thus far been limited; they indicate that water binds molecularly to most smooth crystalline surfaces but dissociates on defect sites.[7−11]

Direct information on the binding orientation of individual water molecules can be hampered by the facile formation of water clusters on the surface due to the high mobility of water molecules on surfaces. In order to obtain information on the interaction of water molecules with a metal surface and, in particular, with well-defined defect sites, the adsorption of water to a metal nanocluster can be studied in the gas phase. Gas-phase experiments on the one hand allow for an unambiguous determination of the number of adsorbed water molecules,

Received: July 22, 2015
Revised: October 8, 2015
Published: October 8, 2015

DOI: 10.1021/acs.jpca.5b07119
J. Phys. Chem. A 2015, 119, 10828–10837

where clusters, a class of matter that bridges the atomic to the bulk, are defect sites by definition: the ability to determine cluster size and its geometric motif offers a level of control over defect sites unattainable for bulk studies. The isolation in the gas phase and in a helium molecular beam environment in particular allows for the stabilization of collision products that are inaccessible in surface studies.

Studies on the interaction of metal ions with water in the gas phase are ample; an overview is given by Beyer.[12] The adsorption of water on metal clusters has drawn considerably less attention, although the adsorption of water onto aluminum clusters has been extensively studied.[13−16] As cobalt in nanoparticulate form plays an important role as a catalyst in the Fischer−Tropsch process,[17,18] there has been a large amount of interest in gas-phase studies of the interaction between cobalt clusters and ligands. Shortly after the development of laser ablation sources,[19,20] the reactivity of neutral cobalt clusters toward water and ammonia was investigated using a flow tube reactor.[21] Thermodynamic information on the interaction between charged cobalt clusters and several ligand molecules has been obtained through mass spectrometric techniques,[22−30] but these do not yield structure-sensitive information.

For this, infrared (IR) photodissociation spectroscopy (IR-PD) has proven to be unsurpassed.[31] In particular, the use of IR free-electron lasers has enabled such studies down to the far-IR region through the absorption of multiple IR photons (IR-MPD).[32] Using this technique, the structures of bare cobalt cluster cations Co_n^+ for sizes up to n = 8 were elucidated.[33] IR spectroscopic information has also been acquired for several ligands bound to cobalt clusters,[34−38] but for water such information is limited to the atomic cation, either solvated by multiple water molecules[39] or in the UV spectral domain.[40] We present here IR spectroscopic data of cationic cobalt clusters, ligated with a single water molecule. The brightness of free-electron laser FELIX allows the probing of photodissociation down to a frequency of 200 cm^{-1}. This provides access to not just the water vibrations but also to vibrations between the water and cluster and of the cluster itself.

Density functional theory (DFT) calculations are usually an integral part in assigning molecular structure to IR spectra. The treatment of transition metal clusters with DFT is, however, challenging as the half filled d-shells may give rise to many possible spin states. For the cobalt studies in this work we note earlier DFT studies[41−45] and in particular the work of Fielicke and co-workers[33] who combined their IR spectral data for cationic cobalt clusters with DFT calculations using the PBE functional.[46] In the current work we use similar computational methods, but focus on the interaction between the cluster and the water molecule.

METHODS

Experimental Section. The experiments described in this paper have been performed using a molecular beam instrument which is coupled to the free electron laser for infrared experiments (FELIX).[47] Cationic clusters are created by pulsed laser ablation of a cobalt sample rod (Goodfellow, purity 99.99%) using the second harmonic of an Nd:YAG laser (532 nm, Brio Quantel, attenuated to 30 mJ per pulse). The sample is rotated and translated by a stepper motor, enabling a homogeneous erosion of the rod. The ablation takes place in a 4-mm-diameter flow-tube-type cluster growth channel in the presence of a helium carrier gas (190 μs, 5−8 bar) that is introduced through a pulsed valve (General Valve, series 9). The pulsed valve is synchronized to the ablation laser to ensure the highest helium density at the time of ablation. The generated plasma and the carrier gas undergo multiple collisions leading to cluster formation. Neutral, anionic, and cationic clusters are created during this process. In order to form cluster−water complexes, a mixture of 1% water vapor in helium is introduced 60 mm downstream into the channel. By adjusting the dosage of the helium−water mixture, it is possible to produce $Co_n^+-(H_2O)_m$ complexes of varying water uptake (m = 1−3). In this study we focus only on the adsorption of one water molecule on cationic cobalt clusters. On exiting the flow reactor, the reaction mixture is expanded into vacuum (10^{-7} mbar), forming a molecular beam. The molecular beam then passes through a 2-mm-diameter skimmer (Beam Dynamics, Inc., model 2) to enter a differentially pumped vacuum chamber and is further shaped by a 1 mm aperture upon entering the extraction region of a mass spectrometer in a third vacuum chamber. Here, the clusters interact with the IR laser beam that is aligned colinearly but is counter propagating with respect to the molecular beam. The focus of the IR beam lies about 25 mm before the extraction point, having a diameter of the same order of magnitude as the molecular beam, thus ensuring that all extracted clusters actually interacted with the IR laser beam.

The IR light is produced by FELIX,[47] which produces intense IR light in the 66−3600 cm^{-1} spectral range; for the present experiments, the range of 200−1700 cm^{-1} is used. The FELIX pulse structure consists of macropulses of 10 μs duration operating at a repetition rate of 10 Hz with a macropulse energy of up to 100 mJ. The macropulse consists of a pulse train of picosecond duration micropulses spaced by 1 ns. The micropulses are transform-limited with a spectral bandwidth that can be adjusted to 0.2−1% RMS of the central frequency; in the current work the bandwidth was kept at 0.3%. A few microseconds after interaction with FELIX, all clusters are extracted by a set of pulsed high-voltage plates into the reflectron time-of-flight mass spectrometer (R. M. Jordan TOF Products, Inc.) and detected with a microchannel plate detector. To correct for long-term source fluctuations, the experiment is operated at twice the FELIX repetition rate, allowing for the recording of reference mass spectra in between successive FELIX pulses. Whenever FELIX is in resonance with a vibrational mode of a given cluster, the number of detected $Co_n^+-H_2O$ cations is reduced due to the dissociation of the complex.

The IR-MPD spectrum is obtained by monitoring the depletion of $Co_n^+-H_2O$ cations as a function of IR frequency. Depletions caused by IR-MPD are expressed as the ratio of the number of ions detected under irradiation with FELIX to that in the reference mass spectrum.

Theoretical. The density functional theory (DFT) calculations reported here have been performed using the 2013 version of the Amsterdam density functional package (ADF2013).[48−50] Previous calculations reported for cationic cobalt clusters are based on the PBE functional,[33,44,45] but in the current work, we decided to describe the exchange-correlation energy with the OPBE functional, a combination of Handy's OPTX modification of the Becke's exchange functional with the Perdew−Burke−Ernzerhof (PBE) correlation functional,[46,51] as OPBE has been used successfully in determining the right spin states for high-spin systems, providing accurate

DOI: 10.1021/acs.jpca.5b07119
J. Phys. Chem. A 2015, 119, 10828−10837

values for the high-spin/low-spin energy splitting for iron complexes.[52−55]

The triple-ζ-type (TZP) basis set from the ADF basis set library is used in which the 1s−2p core for Co atoms as well as the 1s core for the O atom have been kept frozen. To account for relativistic effects, the zeroth-order regular approximation (ZORA) has been used for all calculations.[55,56] SCF convergence of such high-spin systems as cobalt is difficult, but convergence to 10^{-6} is possible in practice in combination with high-accuracy techniques. In some calculations, a mobile block Hessian (MBH) calculation[57,58] was performed in which the relative positions of the cobalt atoms are kept fixed and only the motion of the water relative to the cobalt cluster is considered.

We performed calculations on bare Co_6^+, Co_9^+, and Co_{13}^+ using the initial starting structures of the lowest-energy conformers according to previous studies.[44,45] For every cluster species, a wide range of spin states has been considered to determine the spin state with the lowest energy. As usual in DFT calculations, we hereby define the spin state by the M_S value of the Kohn−Sham determinant, which only rigorously corresponds to the exact spin quantum number for the highest possible spin state of the system.[59]

Minima were verified by frequency calculations with analytical or numerical second derivatives. All energies reported include zero-point energies of all vibrational modes.

Once the stable geometries and spin states of the bare clusters were established, water molecules were added at several trial positions, and the resulting structures were reoptimized in a range of spin states around the lowest-energy spin state found for the bare cluster. To once again establish whether the resulting structures are true minima and, more importantly, to be able to analyze the experimental IR spectra, harmonic frequencies were calculated. All IR spectra reported in this paper have been calculated using analytical frequencies. The accuracy of these calculations was checked by running both numerical and analytical frequency calculations: frequencies calculated using both methods differ by less than 5 cm^{-1}. All frequencies presented in this work are unscaled.

For each optimized complex, a Hirshfeld charge analysis[60] is performed to evaluate the nature of Co_n^+−H_2O bonding. Binding energies are calculated by taking the difference between the energy of the optimized complex and the sum of the unperturbed cluster and water energies, $E_b = E_{cluster-H_2O} - (E_{cluster} + E_{H_2O})$. This value thus includes the energetic cost of possible cluster and water structural rearrangements upon adsorption.

RESULTS AND DISCUSSION

Experiments. Figure 1 shows the experimental IR-MPD spectra of Co_n^+−H_2O clusters in the 200−700 and 1500−1700 cm^{-1} spectral ranges for n = 6−20. Spectra have also been recorded in the 700−1500 cm^{-1} range, but in this range no depletion has been observed. The spectra are presented as the IRMPD intensity I_{IRMPD} defined by

$$I_{IRMPD}(\nu) \approx -\frac{1}{\Phi(\nu)} \ln\left(\frac{I_{IR}(\nu)}{I_{ref}}\right)$$

where $I_{IR}(\nu)$ and I_{ref} represent the ion intensities with FELIX on and off, respectively, and $\Phi(\nu)$ is the photon fluence at frequency ν. Under full power conditions, depletions of up to

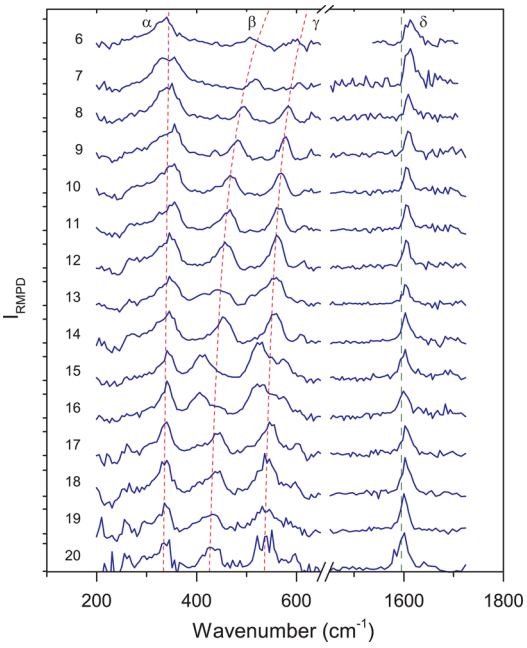

Figure 1. IRMPD spectra of Co_n^+−H_2O (n = 6−20) complexes in the 200−1700 cm^{-1} spectral range. The size dependence of three low-frequency bands is indicated by the red dashed lines; the frequency of the free water bending mode is indicated by the green dashed line.

90% could be achieved. For the reported measurements a compromise between spectral broadening and band visibility has been found for conditions where a maximum depletion of 60% occurred. The spectra in the 200−700 cm^{-1} spectral range are multiplied by a factor of 4 to increase the visibility of the bands.

The spectra exhibit clear resonances in the two spectral regions with widths of several tens of cm^{-1}, which is indicative of a multiple-photon excitation process as suggested in previous experiments.[61] To estimate the number of absorbed photons necessary for dissociation, we consider the bond strength of water to cobalt clusters. The bond strength of water to the cobalt ion (Co^+−H_2O) is measured to be 1.7 eV.[24] While no experimental value is known for clusters, our theoretical calculations on the binding energy of water on Co_n^+ (n = 6,9,13) (vide infra) predict substantially lower values than for the ion. All are higher than 0.33 eV, implying that the absorption of at least two photons at 1600 cm^{-1} and substantially more at lower frequencies is necessary to photodissociate the complex.

It can further be seen that the signal-to-noise ratios reflect the production efficiency: the spectra for the larger clusters are clearly nosier than those in the n = 6−18 range.

As all cluster sizes exhibit a limited number of bands and these bands appear to have a reasonably regular evolution with cluster size, we facilitate the discussion of the resonances by denoting these bands α, β, γ, and δ as indicated in Figure 1. To guide the eye, the evolution of these resonances with size is indicated by dashed red lines. These red lines have been obtained by fitting the observed bands to a Gaussian line shape function; the resulting band centers were subsequently fitted to linear (band α) and hyperbolic (bands β and γ) functions as shown in Figure 2.

All cluster sizes exhibit a resonance around 1600 cm^{-1} (band δ). This band is indicative of the presence of an intact water molecule as it nearly coincides with the bending vibration of

DOI: 10.1021/acs.jpca.5b07119
J. Phys. Chem. A 2015, 119, 10828−10837

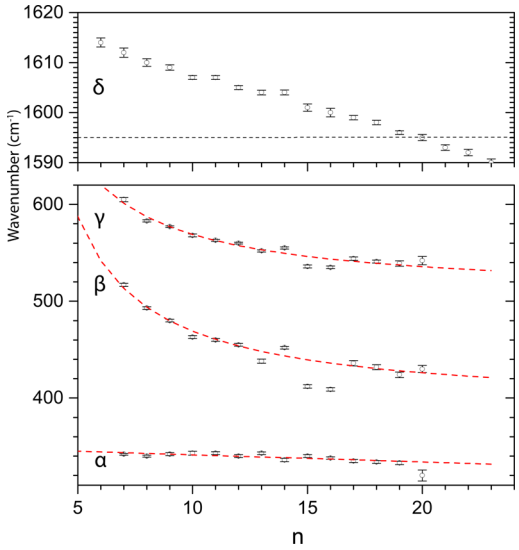

Figure 2. Fitted band centers for the different observed IR resonances and fits to linear and hyperbolic functions. The horizontal dashed line in the top panel indicates the frequency of the free water bending vibration.

free water at 1595 cm^{-1}.[62] The fact that we have observed depletion for the water bending mode of up to 90% at higher IR fluences suggests that for the large majority of species investigated here, water molecules remain intact. Nevertheless, we cannot rule out the presence of dissociated water complexes.

The frequency of the δ band shows a small but clear size dependence as can be seen in Figure 2. One observes that the resonance frequency for smaller cluster sizes exhibits a marked blue shift, which decreases with the cluster size and eventually turns into a slight red shift. This behavior is consistent with other experiments,[63] most notably on V_n^+−H_2O clusters.[64] The blue shifts for the smaller cluster size observed there were attributed to an increase in the H−O−H bond angle caused by a charge transfer induced by the binding of the oxygen atom to the cluster. As a result, electron density on the oxygen is transferred toward the cluster, thereby weakening the H−O bond strength. As the cluster size increases, the transferred charge is redistributed over a larger surface, which is consistent with the decrease in blue shift observed. The red shift for larger clusters, even beyond the free water value of 1595 cm^{-1}, is attributed to the weakening of the O−H bonds. We cannot rule out that the multiphoton techniques used in acquiring the data contribute to the shift. To the best of our knowledge, no value for the water bending mode has been reported for the binding of water to bulk cobalt.

The bands in the lower-frequency range, especially bands β and γ, show a much clearer size dependence. Unlike for the water bending vibration, where vibrational motion is localized entirely in the water molecule, the vibrations expected in this range involve the bond between the cluster and the water molecule. As the reduced mass for this system is size-dependent, the resulting vibrational frequencies will change with size. We will later discuss the exact nature of these modes when we compare the experimental results to the results of the DFT calculations. The regular size evolution of the α, β, and γ bands suggests that the modes are not very sensitive to the cluster structure. In contrast, fluctuations in the δ band indicate a larger sensitivity. A second trend we note is the evolution of the relative intensities for the β and most notably the γ band: the intensities of these bands are very low as compared to those of the α band for n = 6 but gradually become larger, and for the n = 12 cluster they dominate the low-frequency range of the spectrum.

Finally, it is of interest to note that cluster sizes n = 15 and 16 exhibit frequencies that are not very well fitted by the hyperbolic function shown in Figure 2. A closer inspection of the spectra in Figure 1 hints at a splitting of bands β and γ. The cause of this splitting is unknown. Interestingly,[38] there is a report on similar splitting of the N_2 stretching vibration for Co_n^+−N_2 clusters starting at n = 14.

DFT Calculations. DFT calculations have been performed for Co_6^+, Co_9^+, and Co_{13}^+ complexed with water. In all calculated structures the water molecule is, as expected, bound to the positively charged cobalt surface through the binding of the electronegative oxygen to a single Co atom (atop binding). The orientation of the water dipole is not directed completely orthogonal to the surface but certainly is not parallel to the surface as was predicted for the bulk.[5] We find dihedral angles Co−O−H−H on the order of 130−140°. This can be rationalized by the imperfect surface nature of a cluster. All results are collected in Table 1.

Table 1. Stabilization Energies and Binding Energies (in eV), and the Hirshfeld Charge Transfer

species	spin state M_S	E_0	E_b[a]	Δq[b]
6A	13/2	0.23		
	15/2	0.00		
6B	13/2	0.79		
	15/2	[c]		
6A−H_2O	13/2	0.00	−0.83	−0.288
	15/2	0.03	−0.56	−0.238
6B−H_2O				
site 1	13/2	0.70	−0.68	−0.275
site 2	13/2	0.81	−0.58	−0.244
site 3	13/2	0.85	−0.53	−0.245
9A	9	0.00		
9B	9	0.51		
9A−H_2O	9	0.00	−0.64	−0.250
9B−H_2O	9	0.62	−0.57	−0.251
13	15	0.17		
	16	0.00		
13−H_2O	15	0.01	−0.52	−0.247
	16	0.00	−0.34	−0.201

[a] $Eb = E_{(cluster\text{-}H_2O)} - (E_{cluster} + E_{H_2O})$ [b] $\Delta_q = q_{cluster} - q_{H_2O}$ [c] Structure 6B with this spin state relaxes into structure 6A

The nature of the interaction of the cationic cobalt clusters with H_2O can be further studied using an energy decomposition analysis (EDA).[65,66] In this method, the interaction energy between two fragments is split into three physically meaningful components: Pauli repulsion (ΔE_{Pauli}), attractive electrostatic (ΔE_{elstat}), and orbital (ΔE_{orb}) interactions. ΔE_{elstat} gives the electrostatic interaction energy between the fragments, which is calculated with a frozen electron density distribution in the geometry of the complex. The associated orbital term ΔE_{orb} accounts for charge transfer, polarization, and (if applicable) electron-pair bonding. Table 2 shows the energy decomposition for symmetrized Co_6^+ (O_h), Co_9^+ (D_{3h}), and Co_{13}^+ (D_{4h}) clusters interacting with water at the OPBE/

DOI: 10.1021/acs.jpca.5b07119
J. Phys. Chem. A 2015, 119, 10828−10837

Table 2. EDA and QTAIM analysis for $Co_n^+-H_2O$ (n = 6,9,13)

	EDA (eV)					QTAIM (au)	
complex	ΔE_{Pauli}	ΔE_{elstat}	ΔE_{orb}	ΔE_{int}	E_b	ρ	$\nabla^2\rho$
6A−H_2O	2.93	−2.21	−1.61	−0.89	−0.83	0.068	>0
9A−H_2O	1.58	−1.56	−0.64	−0.62	−0.64	0.057	>0
13−H_2O	2.33	−1.83	−0.93	−0.43	−0.52	0.058	>0

TZ2P level of theory. The symmetrization was needed to be able to converge the spin-restricted DFT cobalt clusters that are needed as an intermediate step in the EDA. The final ΔE_{int} includes spin polarization and is, apart from a small geometrical distortion in the latter, identical to the calculations reported in Table 2. From Table 2 we see that the interaction energy decreases in the order $|\Delta E_{int}^{13-H_2O}| < |\Delta E_{int}^{9-H_2O}| < |\Delta E_{int}^{6A-H_2O}|$. This is due to the primarily electrostatic nature of the bonding that decreases in strength as the positive charge on the cobalt cluster is spread out over more atoms. There is no simple trend in the number of atoms; however, for the less symmetric Co_9^+ cluster all three contributions to the interaction energy are relatively small, leading to an energy in between those of the other two. Comparing the very symmetric Co_6^+ and Co_{13}^+ clusters we see that the drop in charge on the frontier cobalt atom from 1/6 e to about 1/13 e correlates well with the factor of 2 decrease in interaction strength. This primarily electrostatic nature of the bonds is also confirmed by a quantum theory of atoms in molecules (QTAIM) analysis.

In Bader's topological analysis,[67] the nature of the bonding is analyzed in terms of the properties of the electron density and its derivatives. The Laplacian of electron density at the bond critical point (BCP), $\nabla^2\rho(r)$, is related to the bond interaction energy by a local expression of the virial theorem $1/4\nabla^2\rho(r) = 2G(r) + V(r)$.[68] The sign of $\nabla^2\rho(r)$ at a BCP is determined by which energy is in present excess over the viral average of 2:1 of kinetics to potential energy. In covalent interactions, the charge density at the BCP is tightly bound and compressed over its average distribution. Therefore, for covalent bonds, a negative value of $\nabla^2\rho(r)$ is expected. On the other hand, in electrostatic interactions the electronic charge is expanded relative to its average distribution. The kinetic energy density is dominant and $\nabla^2\rho(r)$ is positive at the BCP. The computed electron density ρ (r) and Laplacian $\nabla^2\rho(r)$ at the BCPs of selected $Co_n^+-H_2O$ bonds are presented in Table 2. The positive value of $\nabla^2\rho(r)$ at the BCPs indicates that this interaction should indeed be classified as an electrostatic type of bonding. The magnitude of electron densities at the BCPs furthermore correlates well with the trend in interaction energies.

$Co_6^+-H_2O$. For Co_6^+, the two lowest-energy isomers have been investigated: a tetragonal bipyramid (structure 6A) and a capped trigonal bipyramid (structure 6B). Geometries have been taken from ref 33. For structure 6A, the lowest energy is found at a spin state of M_S = 15/2 having bond lengths ranging from 2.24 to 2.33 Å. The same geometry with a spin state of M_S = 13/2 is found 0.23 eV higher in energy with slightly shortened bond lengths. Structure 6B is found at 0.79 eV with a spin state of M_S = 13/2. These calculated results are in good agreement with previous DFT studies.[33,44,45]

Because of its highly symmetric shape, only one water adsorption site on the surface has been calculated for structure 6A. The addition of water onto 6A strongly reduces the energy difference between the lowest spin states: the energies of 6A−H_2O complexes with M_S = 13/2 and 15/2 are almost identical (0 and 0.03 eV, respectively). This is reflected in a substantially larger binding energy of 0.83 eV for water on the M_S = 13/2 surface against 0.56 eV on the M_S = 15/2 surface.

For the capped trigonal bipyramid (6B), several water adsorption sites (6B-1, 6B-2, and 6B-3) have been tested (Figure 3). The lowest-energy structures are all found for a spin

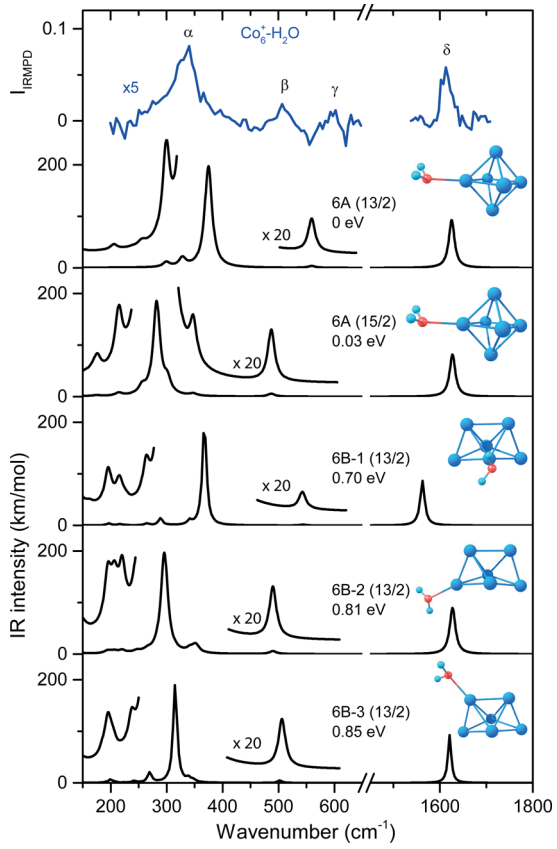

Figure 3. Experimental spectrum of $Co_6^+-H_2O$ compared to calculated IR spectra of the lowest -energy structures of 6A and 6B. Each calculated spectrum is accompanied by the structure name, spin state M_S (in parentheses), and its relative energy (including zero-point energy).

state with M_S = 13/2. In absolute terms, they are all found at energies of 0.7−0.85 eV above that of the 6A−water complex. It is further noteworthy that 6B−1 and 6B−2 relax into 6A−water on the M_S = 15/2 surface, as does the bare cluster itself.

The calculated spectra for selected structures are shown together with the experimental results in Figure 3. The calculated IR spectra have been convoluted with a Lorentzian line shape function with a 15 cm^{-1} width. The experimental spectrum of $Co_6^+-H_2O$ shows four distinct peaks centered at 331, 501, 590, and 1614 cm^{-1}. The α and δ bands are the most intense and have widths of 68 and 26 cm^{-1} (fwhm), respectively. The β and γ bands are much weaker, with associated widths of 45 and 35 cm^{-1}, respectively.

All calculated IR spectra predict a number of vibrational modes below 300 cm^{-1} with IR intensities of less than 20 km/mol and associated with internal cluster vibrations. Each calculated spectrum is dominated by two very intense bands: the water bending vibration close to 1600 cm^{-1} and the water wagging vibration. The line position of the latter varies considerably for 6A, ranging from 282 cm^{-1} at M_S = 15/2 to 325 cm^{-1} at M_S = 13/2. Values for 6B are found in between

DOI: 10.1021/acs.jpca.5b07119
J. Phys. Chem. A 2015, 119, 10828−10837

these extremes. Most structures exhibit two minor bands in between the two high-intensity bands. The highest-frequency mode of these is in all cases the rocking motion of the water molecule. A zoom-in on this part of the spectrum shows their presence, with calculated IR intensities lower than 10 km/mol.

Although in agreement with the experimental observation that each calculated spectrum displays a strong band, the overall match between calculated and observed spectra in the 200−600 cm^{-1} spectral range is not very good. The observed mismatch in predicted and observed frequency of the strong band should not be of too much concern: in most theoretical calculations, the harmonic frequencies reported are typically overestimated in comparison to observed values. This discrepancy is attributed to the fact that the theoretical treatment does not take anharmonicity into account. In most cases, the discrepancies are found to be uniform and can be corrected for by empirical scaling factors so that good agreement between theory and experiment can be obtained.[69] In the present case, the concern is rather that none of the calculated spectra exhibit the reasonably intense β and γ bands. Although the calculations predict bands to the blue of the α band, they are very weak and their frequency does not match the experimentally observed frequencies. Of course, the signal-to-noise ratio for the β and γ bands is not as good as for the α band, but their visibility for larger cluster sizes is much better and calculations do not predict these either, as will become clear below.

One could speculate that the problem is caused by the density functional that is employed; a common strategy is then to carry out calculations with other functionals as well and check for qualitative differences. In order to do so, we carried out calculations using different functionals for three different spin states of Co_6^+−H_2O. We chose the revised Perdew−Burke−Ernzerhof (revPBE) functional in the generalized gradient approximation (GGA),[46] with which the spectral assignment of bare cationic cobalt clusters was performed,[33] and the Tao−Perdew−Staroverov−Scuseria (TPSS) functional in the meta-generalized gradient approximation (Meta-GGA).[70] With the latter we have recently been able to assign the spectra for neutral cobalt clusters.[71] To test whether a dispersion-corrected density functional has an influence on the vibrational frequencies, we included calculations with the OPBE functional corrected with the D3 method of Grimme.[72] All calculations make use of the same TZ2P basis set. The results of these calculations are depicted in Figure 4. As in all other figures, no frequency scaling is applied. The results show that recomputed spectra vary substantially in line positions but not in their failure to predict the relatively high intensities of the β and γ modes. Thus, this is likely to be a general feature of the use of harmonic frequencies calculated at the minima of the potential energy surface.

On the basis of these calculations we can neither assign our spectrum to a specific structure nor give a verdict on which of the used functionals is the most accurate. We continue for the moment our use of OPBE for harmonic frequency calculations, but we will later discuss the purported failure of the spectral predictions in more detail.

Co_9^+−H_2O. For our calculations on bare Co_9^+, we have started from the geometry of the lowest-energy structure as predicted by previous theoretical studies.[44,45] These are the tricapped trigonal prism (9A) and the bicapped pentagonal bipyramid (9B), for both of which a spin state of $M_S = 9$ turns out to give the lowest energies, with 9B being less stable by 0.51 eV. Co−Co bond lengths found range from 2.24 to 2.52 Å for

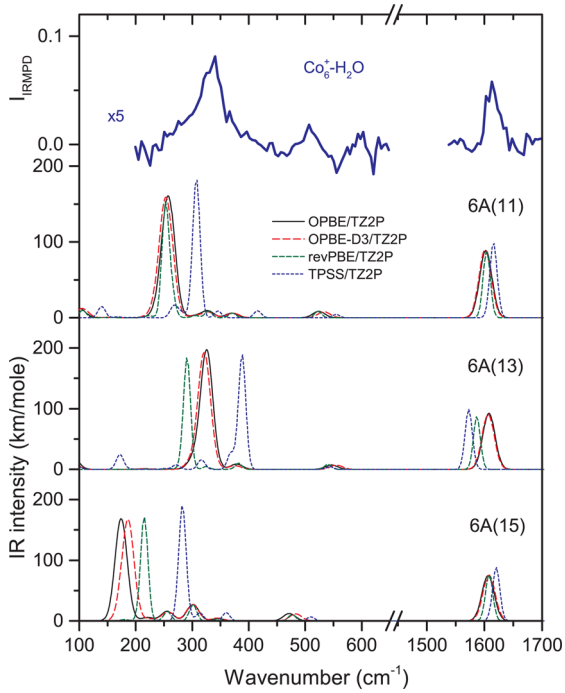

Figure 4. Comparison of the experimental spectrum of Co_6^+−H_2O to theoretical spectra for structure 6A calculated with different theoretical methods.

9A and from 2.22 to 2.35 Å for 9B. Different spin states around this minimum structure have energies about 1 eV higher. Onto these stable structures water is added, and the structure is reoptimized for different spin states. The results in Table 1 show that the interaction of H_2O with both 9A and 9B does not change the spin state; the average O−H and Co−Co bond lengths and the H−O−H bond angle, on the other hand, increase slightly upon complexation.

The experimental spectrum (top panel in Figure 5) displays four distinct peaks centered around 342, 480, 577, and 1609

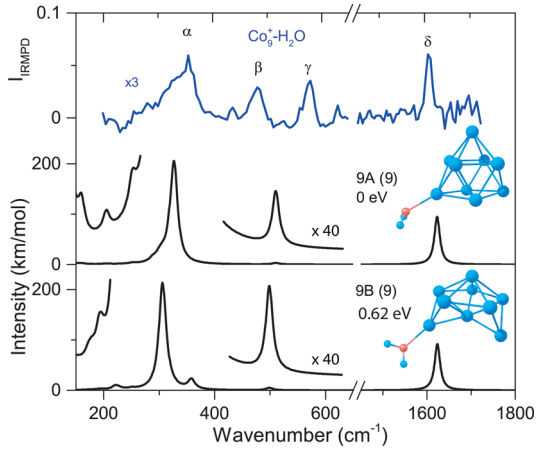

Figure 5. Comparison of the experimental IRMPD spectrum of the Co_9^+−H_2O cluster with the computed spectra for different structures.

cm^{-1}. The theoretical spectra exhibit a similar trend as for Co_6^+−H_2O: an intense band near 300 cm^{-1} and only weak features to the blue of this band, in clear disagreement with experimental findings. The calculated spectra appear to be less sensitive to changes in the spin state than for Co_6^+−H_2O; the

DOI: 10.1021/acs.jpca.5b07119
J. Phys. Chem. A 2015, 119, 10828−10837

energy difference between 9A and 9B is substantial at 0.62 eV. Binding energies found for 9A and 9B are 0.64 and 0.57 eV, respectively.

Co_{13}^{+}–H_2O. Calculations for Co_{13}^{+} have been made using the cluster geometry found in ref 44. The most stable structures found have spin states of M_S = 15 and 16, where the higher spin state is favored by 0.17 eV. The binding energies of water to Co_{13}^{+} (M_S = 15) is computed at 0.52 eV, and that for M_S = 16 is even lower at 0.34 eV, making the M_S = 16 structure the lowest in energy, albeit by a meager 0.01 eV. Both binding energies are substantially lower than the binding energies found for the Co_6^{+} and Co_9^{+} clusters. This can be rationalized by taking into account that in the icosahedral structure each atom is coordinated to five neighboring atoms. It also implies that at 1600 cm^{-1} only two photons need to be absorbed to induce dissociation.

The experimental spectra (Figure 6) follow the trend observed before: an intense band at 343 cm^{-1} and at least

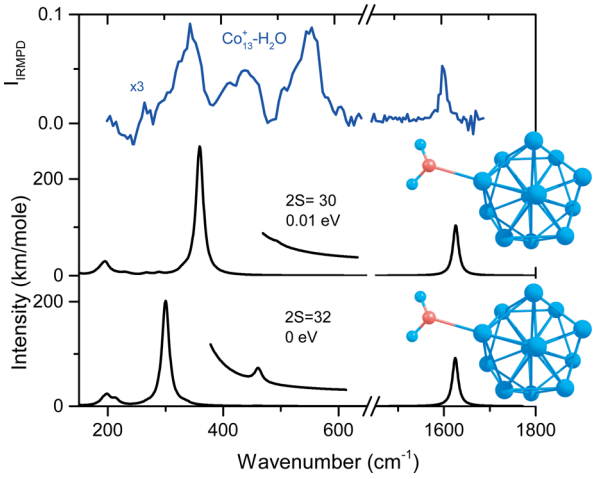

Figure 6. Comparison of the experimental IRMPD spectrum of the Co_{13}^{+}–H_2O cluster with the computed spectra for different structures.

two bands at frequencies of between 400 and 600 cm^{-1} (band centers at 438 and 552 cm^{-1}, respectively). Interestingly, we now find that the band at 552 cm^{-1} is more intense than the band we tentatively assign to the wagging vibration at 343 cm^{-1}. The calculated spectra for different spin states are nearly identical apart from a substantial shift of the frequency of the wagging vibration. As observed before, the predicted intensities of the higher-frequency modes do not agree with the experimental observations.

Discussion. The results from the previous sections show that the harmonic calculations do not provide a qualitatively correct description of the observed spectra: where the predicted frequencies and IR intensities for the water bending mode (around 1600 cm^{-1}) are quite reasonable, those predicted for the water–cluster vibrations are inadequate as they simply fail to reproduce the number of intense IR bands observed in the experiments. To rule out any effects from the choice of functional, we carried out the same calculations for Co_6^{+}–H_2O using two different functionals. The results suggest that OPBE is not performing worse than OPBE-D3, revPBE, or TPSS: there are differences in frequencies and intensities, but neither method offers a better prediction of the intensities of the β and γ bands.

All methods reasonably agree on the nature of the vibrations calculated, which are schematically shown in Figure 7. The

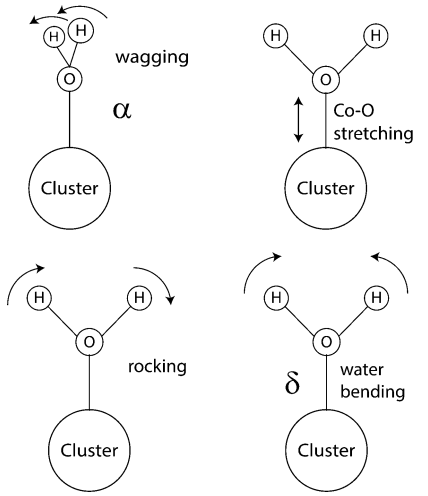

Figure 7. Schematic representation of theoretically predicted vibrational modes.

most intense band is the water libration mode, where the water molecule makes a wagging motion. We tentatively assign the α bands, being the most intense bands observed, to this vibration. A second much more definite assignment is the water bending mode to the δ bands. For the β and γ bands none of the calculations offer a satisfactory prediction. Frequencies do not match, and the intensities are very low. They also give no indication of an increase in intensity with growing cluster size.

One may argue that IR-MPD spectra should not be compared to the (calculated) linear absorption spectrum. It is true that IR intensities are not always represented well, but usually the frequencies are predicted quite accurately. In the present case, the intensities are very different, and no clear trend is found in the frequency of modes upon enlarging the number of Co atoms in the cluster. Given the regularity in the frequency evolution with cluster size, it is, however, tempting to conclude that the exact cluster geometry is subservient to the Co–O bond involving the single Co atom and that the cluster size effectively comes in only to modify the reduced mass involved in the vibration.

To test this hypothesis we carry out two types of calculations. In the first we calculate the analytical Hessian to obtain the IR spectrum for Co^{+}–H_2O and then calculate the equivalent for isotopically substituted analogues, taking the mass of Co_n. The results of these calculation are shown in panel a of Figure 8. As a single atom will also be electronically quite different from a cluster, we also repeat this calculation for structure 6A, where we show the results of a similar isotopic substitution in Figure 8b. In a second type of calculation we employ the mobile block Hessian (MBH) approach to freeze the internal degrees of freedom of the Co clusters, letting the cluster move as one heavy atom. Together these calculations allow a separation of the electronic effect of enlarging the cobalt cluster versus the increase in the mass of the cluster.

Calculations of Co^{+}–H_2O yield a structure characterized by a 1.925 Å Co–O bond length and a 142.5° Co–O–H–H dihedral angle. The bond length found is slightly shorter than that for the $^3B_2$ structure reported in ref 73 (1.992 Å). Of its six vibrations, the four in the presently studied spectral region are

DOI: 10.1021/acs.jpca.5b07119
J. Phys. Chem. A 2015, 119, 10828–10837

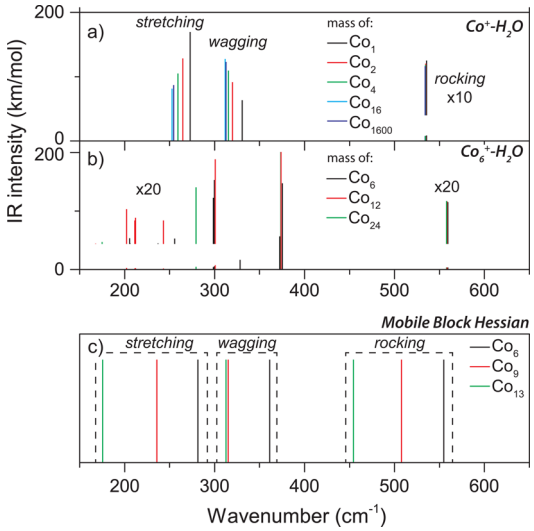

Figure 8. Two methods attempting to separate cluster and cluster–water vibrations: isotopic substitution of Co^+ (a) and 6A (b) and frozen-block calculations for structures 6A, 9A, and 13 found above (c).

the water bending mode (1582 cm^{-1}), the Co–O stretching mode (425 cm^{-1}), and two water libration modes (wagging at 313 cm^{-1}, and rocking at 642 cm^{-1}). As expected, the three low-frequency modes shift toward the red for an increasing cobalt mass, but it is striking that the water bending mode and the rocking mode barely shift. At the same time, the relative IR intensities for the two lower-frequency modes change substantially. The isotopic substitution of the calculated spectrum for 6A offers less clear trends. The wagging mode red shifts but only marginally, whereas the rocking mode is virtually unchanged. In both cases the change in mass alone does not explain the experimental observation of strongly red-shifted β and γ peaks that are both increasing in intensity.

In the MBH calculations, we consider the minima found for 6A, 9A, and 13 as shown in Figure 8. Unfortunately intensities are not yet implemented for this method, so we can discuss only the position of the peaks. Here, we discern substantial red shifts for all three low-frequency vibrations (stretching, wagging, and rocking) with mass. In particular, for the problematic γ bands it is the first time we observe a substantial shift. However, the shift of the wagging mode is now larger than observed in the experiments, and assuming that the stretching mode is not responsible for the α band, the third β band is not predicted either.

It is obvious that the simple qualitative models discussed above are not accurate enough for the current problem. However, they do to some extent exhibit the systematic shifts that we observe in the experimental spectra. While they certainly do not match the observed spectra, the size-dependent shifts reinforce our suspicions that the water–cobalt coupling is less strong than the calculations for the optimized geometries suggest.

A possible cause of the discrepancy is the shallowness of the potential energy surface relating to the Co–H_2O bond, which gives rise to rather anharmonic potentials that can invalidate the harmonic approximation used to compute the frequencies. Moreover, at the temperature at which the experiments are carried out this fluctional system may actually sample a larger region of the potential energy surface than is described by the local minima only. In such regions away from the minima, local dipole moments may change rapidly, leading to much stronger absorption intensities. Exploratory calculations at geometries that are slightly distorted along the lowest-energy vibrational coordinates (torsions of the Co–O bond or slight water displacements) indeed already show a large influence on both frequencies and IR intensities.

One way to improve the current calculations is thus the implementation of methods that sample not just the potential minimum but a larger part of the potential energy well. Recently, Born–Oppenheimer molecular dynamics (BOMD) were successfully implemented to describe the very anharmonic vibrations probed in small peptide model systems.[74] However, for the problem at hand the implementation of such calculations is not expected to be trivial, given the proximity of different spin surfaces.

CONCLUSIONS

We have recorded the IR spectra for cationic cobalt clusters complexed with water molecules, Co_n^+–H_2O (n = 6–20), using IR-MPD spectroscopy. These constitute the first spectra of water adsorbed onto transition-metal clusters that directly address the vibrations of the water–cluster bond; one earlier study of water adsorbed onto vanadium clusters investigated only the vibration of the water itself.[64] The experimental spectra provide clear resonances in the 200–600 cm^{-1} spectral range that are evolving quite regularly with cluster size.

The deceiving simplicity of the size-evolution of the observed bands is all the more intriguing as the theoretical description using harmonic frequencies at the OPBE/TZP level is accurate for the localized water bending mode near 1600 cm^{-1} but interestingly appears to fail in the low-frequency range. We have investigated whether the use of other functionals OPBE-D3, revPBE, or TPSS) improves the description, but we found no large improvements. Factors that may play a role in this are a possible overestimation of the coupling strength between water–cluster motions and internal cluster vibrations or a strongly anharmonic shape of the potential well of the Co–H_2O bond.

As the current data are the first that directly probe the interaction between cobalt clusters and water, they can serve as a benchmark for future developments in describing the metal–water bond which is of fundamental importance. At the same time it is clear that extending these types of studies to other metals will further our understanding of such bonds. Such studies are therefore currently being pursued in our laboratory.

AUTHOR INFORMATION

Corresponding Author

*E-mail: J.Bakker@science.ru.nl.

Notes

The authors declare no competing financial interest.

ACKNOWLEDGMENTS

We gratefully acknowledge the Stichting voor Fundamenteel Onderzoek der Materie (FOM) for the support of the FELIX Laboratory. D.M.K. acknowledges financial support from Nederlandse Organisatie voor Wetenschappelijk Onderzoek (NWO Chemical Sciences) as part of the to Dutch Astrochemistry Network (grant 648.000.006). We are grateful for the skillful technical support provided by the entire FELIX staff, in particular, Dr. A. F. G. van der Meer and Dr. B. Redlich.

DOI: 10.1021/acs.jpca.5b07119
J. Phys. Chem. A 2015, 119, 10828–10837

We finally thank U. van Hes and M. Hilbers for the construction of the laser ablation source. We thank NWO Physical Sciences (EW) and the SurfSara Supercomputer Center for providing the computational resources. JO thanks the Stichting Physica for support.

REFERENCES

(1) Thiel, P. A.; Madey, T. E. The Interaction of Water With Solid Surfaces: Fundamental Aspects. *Surf. Sci. Rep.* **1987**, *7*, 211−385.
(2) Henderson, M. The Interaction of Water With Solid Surfaces: Fundamental Aspects Revisited. *Surf. Sci. Rep.* **2002**, *46*, 1−308.
(3) Hodgson, A.; Haq, S. Water Adsorption and the Wetting of Metal Surfaces. *Surf. Sci. Rep.* **2009**, *64*, 381−451.
(4) Carrasco, J.; Hodgson, A.; Michaelides, A. A Molecular Perspective of Water at Metal Interfaces. *Nat. Mater.* **2012**, *11*, 667−674.
(5) Michaelides, A.; Ranea, V.; de Andres, P.; King, D. General Model for Water Monomer Adsorption on Close-Packed Transition and Noble Metal Surfaces. *Phys. Rev. Lett.* **2003**, *90*, 216102.
(6) Motobayashi, K.; Matsumoto, C.; Kim, Y.; Kawai, M. Vibrational Study of Water Dimers on Pt(111) Using a Scanning Tunneling Microscope. *Surf. Sci.* **2008**, *602*, 3136−3139.
(7) Moyes, R. B.; Roberts, M. W. Interaction of Cobalt With Oxygen, Water Vapor, and Carbon Monoxide 1X-Ray and Ultraviolet Photo Emission Studies. *J. Catal.* **1977**, *49*, 216−224.
(8) Heras, J.; Albano, E. Work Function Changes of Cobalt Films at 77 K Upon Water Adsorption. *Appl. Surf. Sci.* **1981**, *7*, 332−346.
(9) Heras, J.; Papp, H.; Spiess, W. Face Specificity of the H_2O Adsorption and Decomposition on Co Surfaces a LEED, UPS, SP and TPD Study. *Surf. Sci. Lett.* **1982**, *117*, A219.
(10) Grellner, F.; Klingenberg, B.; Borgmann, D.; Wedler, G. Interaction of H_2O with Co(1120): a Photoelectron Spectroscopic Study. *Surf. Sci.* **1994**, *312*, 143−150.
(11) Xu, L.; Ma, Y.; Zhang, Y.; Chen, B.; Wu, Z.; Jiang, Z.; Huang, W. Water Adsorption on a Co(0001) Surface. *J. Phys. Chem. C* **2010**, *114*, 17023−17029.
(12) Beyer, M. K. Hydrated Metal Ions in the Gas Phase. *Mass Spectrom. Rev.* **2007**, *26*, 517−541.
(13) Cox, D. M.; Trevor, D. J.; Whetten, R. L.; Kaldor, A. Aluminum Clusters: Ionization Thresholds and Reactivity toward Deuterium, Water, Oxygen, Methanol, Methane, and Carbon Monoxide. *J. Phys. Chem.* **1988**, *92*, 421−429.
(14) Lippa, T.; Lyapustina, S.; Xu, S.-J.; Thomas, O.; Bowen, K. Magic Numbers in $Al_n^+(H_2O)_1$ Cluster Cations. *Chem. Phys. Lett.* **1999**, *305*, 75−78.
(15) Roach, P. J.; Woodward, W. H.; Castleman, A. W., Jr.; Reber, A. C.; Khanna, S. N. Complementary Active Sites Cause Size-Selective Reactivity of Aluminum Cluster Anions with Water. *Science* **2009**, *323*, 492−495.
(16) Reber, A. C.; Khanna, S. N.; Roach, P. J.; Woodward, W. H.; Castleman, A. W., Jr. Reactivity of Aluminum Cluster Anions With Water: Origins of Reactivity and Mechanisms for H_2 Release. *J. Phys. Chem. A* **2010**, *114*, 6071−6081.
(17) Bezemer, G. L.; Bitter, J. H.; Kuipers, H. P. C. E.; Oosterbeek, H.; Holewijn, J. E.; Xu, X.; Kapteijn, F.; van Dillen, J.; de Jong, K. P. Cobalt Particle Size Effects in the Fischer−Tropsch Reaction Studied with Carbon Nanofiber Supported Catalysts. *J. Am. Chem. Soc.* **2006**, *128*, 3956−3964.
(18) Khodakov, A. Y.; Chu, W.; Fongarland, P. Advances in the Development of Novel Cobalt Fischer−Tropsch Catalysts for Synthesis of Long-Chain Hydrocarbons and Clean Fuels. *Chem. Rev.* **2007**, *107*, 1692−1744.
(19) Dietz, T. G.; Duncan, M.; Powers, D.; Smalley, R. Laser Production of Supersonic Metal Cluster Beams. *J. Chem. Phys.* **1981**, *74*, 6511−6512.
(20) Bondybey, V. E.; English, J. H. Laser-Induced Fluorescence of Metal-Clusters Produced by Laser Vaporization Gas-Phase Spectrum of Pb_2. *J. Chem. Phys.* **1981**, *74*, 6978−6979.
(21) Parks, E. K.; Klots, T. D.; Winter, B. J.; Riley, S. J. Reactions of Cobalt Clusters with Water and Ammonia: Implications for Cluster Structure. *J. Chem. Phys.* **1993**, *99*, 5831−5839.
(22) Nakajima, A.; Kishi, T.; Sone, Y.; Nonose, S.; Kaya, K. Reactivity of Positively Charged Cobalt Cluster Ions With CH_4, N_2, H_2, C_2H_4, and C_2H_2. *Z. Phys. D: At., Mol. Clusters* **1991**, *19*, 385−387.
(23) Hales, D. A.; Su, C.-X.; Lian, L.; Armentrout, P. B. Collision-Induced Dissociation of Co^+_n (n = 2−18) With Xe: Bond Energies of Cationic and Neutral Cobalt Clusters, Dissociation Pathways, and Structures. *J. Chem. Phys.* **1994**, *100*, 1049−1057.
(24) Dalleska, N. F.; Honma, K.; Sunderlin, L. S.; Armentrout, P. B. Solvation of Transition Metal Ions by Water. Sequential Binding Energies of $M^+(H_2O)_x$ (x = 1−4) for M = Ti to Cu Determined by Collision-Induced Dissociation. *J. Am. Chem. Soc.* **1994**, *116*, 3519−3528.
(25) Kapiloff, E.; Ervin, K. M. Reactions of Cobalt Cluster Anions with Oxygen, Nitrogen, and Carbon Monoxide. *J. Phys. Chem. A* **1997**, *101*, 8460−8469.
(26) Øiestad, A.; Leere, M.; Uggerud, E. Gas Phase Reactivity of Small Cationic Cobalt Clusters Towards Methanol. *Chem. Phys.* **2000**, *262*, 169−177.
(27) Liu, F.; Armentrout, P. B. Guided Ion-Beam Studies of the Kinetic-Energy-Dependent Reactions of Co_n^+(n = 2−16) with D_2: Cobalt Cluster-Deuteride Bond Energies. *J. Chem. Phys.* **2005**, *122*, 194320.
(28) Hanmura, T.; Ichihashi, M.; Kondow, T. Chemisorption of Nitrogen Monoxide on Size-Selected Cobalt Cluster Ions. *Isr. J. Chem.* **2007**, *47*, 37−42.
(29) Citir, M.; Liu, F.; Armentrout, P. B. Methane Activation by Cobalt Cluster Cations, Co_n (n = 2−16): Reaction Mechanisms and Thermochemistry of Cluster-$(CH)_x$ (x = 0−3) Complexes. *J. Chem. Phys.* **2009**, *130*, 054309.
(30) Poisson, L.; Dukan, L.; Sublemontier, O.; Lepetit, F.; Reau, F.; Pradel, P.; Mestdagh, J.-M.; Visticot, J. Probing Several Structures of $Fe(H_2O)_n^+$ and $Co(H_2O)_n^+$ (n = 1−10) Cluster Ions. *Int. J. Mass Spectrom.* **2002**, *220*, 111−126.
(31) Duncan, M. A. Infrared Spectroscopy to Probe Structure and Dynamics in Metal Ion−Molecule Complexes. *Int. Rev. Phys. Chem.* **2003**, *22*, 407−435.
(32) Fielicke, A.; Kirilyuk, A.; Ratsch, C.; Behler, J.; Scheffler, M.; von Helden, G.; Meijer, G. Structure Determination of Isolated Metal Clusters via Far-Infrared Spectroscopy. *Phys. Rev. Lett.* **2004**, *93*, 023401.
(33) Gehrke, R.; Gruene, P.; Fielicke, A.; Meijer, G.; Reuter, K. Nature of Ar Bonding to Small Co_n^+ Clusters and its Effect on the Structure Determination by Far-Infrared Absorption Spectroscopy. *J. Chem. Phys.* **2009**, *130*, 034306.
(34) Swart, I.; Fielicke, A.; Rayner, D. M.; Meijer, G.; Weckhuysen, B. M.; de Groot, F. M. F. Controlling the Bonding of CO on Cobalt Clusters by Coadsorption of H_2. *Angew. Chem., Int. Ed.* **2007**, *46*, 5317−5320.
(35) Swart, I.; de Groot, F. M. F.; Weckhuysen, B. M.; Gruene, P.; Meijer, G.; Fielicke, A. H_2 Adsorption on 3d Transition Metal Clusters: A Combined Infrared Spectroscopy and Density Functional Study. *J. Phys. Chem. A* **2008**, *112*, 1139−1149.
(36) Hirabayashi, S.; Okawa, R.; Ichihashi, M.; Kawazoe, Y.; Kondow, T. Structures and Reactions of Methanol Molecules on Cobalt Cluster Ions Studied by Infrared Photodissociation Spectroscopy. *J. Chem. Phys.* **2009**, *130*, 164304.
(37) Bialach, P. M.; Funk, A.; Weiler, M.; Gerhards, M. IR Spectroscopy on Isolated Co_n−$(alcohol)_m$ Cluster Anions (n = 1−4,m = 1−3): Structures and Spin States. *J. Chem. Phys.* **2010**, *133*, 194304.
(38) Dillinger, S.; Mohrbach, J.; Hewer, J.; Gaffga, M.; Niedner-Schatteburg, G. Infrared Spectroscopy of N_2 Adsorption on Size Selected Cobalt Cluster Cations in Isolation. *Phys. Chem. Chem. Phys.* **2015**, *17*, 10358−10362.
(39) Furukawa, K.; Ohashi, K.; Koga, N.; Imamura, T.; Judai, K.; Nishi, N.; Sekiya, H. Coordinatively Unsaturated Cobalt Ion in

DOI: 10.1021/acs.jpca.5b07119
J. Phys. Chem. A 2015, 119, 10828−10837

$Co^+(H_2O)_n$ (n = 4−6) Probed With Infrared Photodissociation Spectroscopy. *Chem. Phys. Lett.* **2011**, *508*, 202−206.
(40) Kocak, A.; Austein-Miller, G.; Pearson, W. L.; Altinay, G.; Metz, R. B. Dissociation Energy and Electronic and Vibrational Spectroscopy of $Co^+(H_2O)$ and its Isotopomers. *J. Phys. Chem. A* **2013**, *117*, 1254−1264.
(41) Ogasawara, H.; Brena, B.; Nordlund, D.; Nyberg, M.; Pelmenschikov, A.; Pettersson, L.; Nilsson, A. Structure and Bonding of Water on Pt(111). *Phys. Rev. Lett.* **2002**, *89*, 276102.
(42) Lee, E. P.; Almahdi, Z.; Musgrave, A.; Wright, T. G. Structures and Binding Energies of K^+-H_2O, K^+-CO_2 and K^+-N_2. *Chem. Phys. Lett.* **2003**, *373*, 599−605.
(43) Gutsev, G.; Mochena, M.; Bauschlicher, C. Interaction of Water With Small Fe_n Clusters. *Chem. Phys.* **2005**, *314*, 291−298.
(44) Datta, S.; Kabir, M.; Ganguly, S.; Sanyal, B.; Saha-Dasgupta, T.; Mookerjee, A. Structure, Bonding, and Magnetism of Cobalt Clusters From First-Principles Calculations. *Phys. Rev. B: Condens. Matter Mater. Phys.* **2007**, *76*, 014429.
(45) Rodriguez-Lopez, J. L.; Aguilera-Granja, F.; Michaelian, K.; Vega, A. Structure and Magnetism of Cobalt Clusters. *Phys. Rev. B: Condens. Matter Mater. Phys.* **2003**, *67*, 174413.
(46) Perdew, J. P.; Burke, K.; Ernzerhof, M. Generalized Gradient Approximation Made Simple [Phys. Rev. Lett. 77, 3865 (1996)]. *Phys. Rev. Lett.* **1997**, *78*, 1396−1396.
(47) Oepts, D.; van der Meer, A. F. G.; van Amersfoort, P. The Free-Electron-Laser User Facility FELIX. *Infrared Phys. Technol.* **1995**, *36*, 297−308.
(48) te Velde, G.; Bickelhaupt, F. M.; Baerends, E. J.; Fonseca Guerra, C.; van Gisbergen, S. J. A.; Snijders, J. G.; Ziegler, T. Chemistry with ADF. *J. Comput. Chem.* **2001**, *22*, 931−967.
(49) Fonseca Guerra, C.; Snijders, J. G.; te Velde, G.; Baerends, E. J. Towards an Order- N DFT Method. *Theor. Chim. Acta* **1998**, *99*, 391−403.
(50) Baerends, E. J.; Ziegler, J.; Autschbach, D.; Bashford, A.; Bérces, F.; Bickelhaupt, C.; Bo, P.; Boerrigter, L.; Cavallo, D. et al. *ADF2013, SCM, Theoretical Chemistry*; Vrije Universiteit, Amsterdam, The Netherlands, www.scm.com, 2013; accessed February 1, 2014.
(51) Handy, N. C.; Cohen, A. J. Left-Right Correlation Energy. *Mol. Phys.* **2001**, *99*, 403−412.
(52) Swart, M.; Groenhof, A. R.; Ehlers, A. W.; Lammertsma, K. Validation of Exchange Correlation Functionals for Spin States of Iron Complexes. *J. Phys. Chem. A* **2004**, *108*, 5479−5483.
(53) Ganzenmüller, G.; Berkaïne, N.; Fouqueau, A.; Casida, M. E.; Reiher, M. Comparison of Density Functionals for Differences Between the High- (5T2g) and Low- (1A1g) Spin States of Iron(II) Compounds. IV. Results for the Ferrous Complexes [Fe-('NHS4')]. *J. Chem. Phys.* **2005**, *122*, 234321.
(54) Conradie, J.; Ghosh, A. Electronic Structure of Trigonal-Planar Transition-Metal-Imido Complexes: Spin-State Energetics, Spin-Density Profiles, and the Remarkable Performance of the OLYP Functional. *J. Chem. Theory Comput.* **2007**, *3*, 689−702.
(55) Pierloot, K.; Vancoillie, S. Relative Energy of the High-(5T2g) and Low-(1A1g) Spin States of the Ferrous Complexes [Fe(L)(NHS4)]: CASPT2 Versus Density Functional Theory. *J. Chem. Phys.* **2008**, *128*, 034104.
(56) van Lenthe, E.; Snijders, J. G.; Baerends, E. J. The Zero-Order Regular Approximation for Relativistic Effects: The Effect of Spin Orbit Coupling in Closed Shell Molecules. *J. Chem. Phys.* **1996**, *105*, 6505−6516.
(57) Ghysels, A.; van Neck, D.; van Speybroeck, V.; Verstraelen, T.; Waroquier, M. Vibrational Modes in Partially Optimized Molecular Systems. *J. Chem. Phys.* **2007**, *126*, 224102.
(58) Ghysels, A.; van Neck, D.; Waroquier, M. Cartesian Formulation of the Mobile Block Hessian Approach to Vibrational Analysis in Partially Optimized Systems. *J. Chem. Phys.* **2007**, *127*, 164108.
(59) Jacob, C. R.; Reiher, M. Spin in Density-Functional Theory. *Int. J. Quantum Chem.* **2012**, *112*, 3661−3684.
(60) Hirshfeld, F. L. Bonded-Atom Fragments for Describing Molecular Charge Densities. *Theor. Chim. Acta* **1977**, *44*, 129−138.
(61) Oomens, J.; Sartakov, B. G.; Meijer, G.; von Helden, G. Gas-Phase Infrared Multiple Photon Dissociation Spectroscopy of Mass-Selected Molecular Ions. *Int. J. Mass Spectrom.* **2006**, *254*, 1−19.
(62) Toth, R. A. Water Vapor Measurements Between 590 and 2582 cm^{-1}: Line Positions and Strengths. *J. Mol. Spectrosc.* **1998**, *190*, 379−396.
(63) Fielicke, A.; von Helden, G.; Meijer, G.; Pedersen, D. B.; Simard, B.; Rayner, D. M. Size and Charge Effects on the Binding of CO to Late Transition Metal Clusters. *J. Chem. Phys.* **2006**, *124*, 194305.
(64) Jaeger, T.; Fielicke, A.; von Helden, G.; Meijer, G.; Duncan, M. Infrared Spectroscopy of Water Adsorption on Vanadium Cluster Cations V_x^+; (x = 3−18). *Chem. Phys. Lett.* **2004**, *392*, 409−414.
(65) Morokuma, K. Molecular Orbital Studies of Hydrogen Bonds. III. C═O···H−O Hydrogen Bond in $H_2CO···H_2O$ and $H_2CO···_2H_2O$. *J. Chem. Phys.* **1971**, *55*, 1236−1244.
(66) Ziegler, T.; Rauk, A. On the Calculation of Bonding Energies by the Hartree Fock Slater Method. *Theor. Chim. Acta* **1977**, *46*, 1−10.
(67) Bader, R. F. W. A Q Theory of Molecular Structure and its Applications. *Chem. Rev.* **1991**, *91*, 893−928.
(68) Bader, R. *Atoms in Molecules: A Quantum Theory*; University Press: Oxford, 1990.
(69) Scott, A. P.; Radom, L. *J. Phys. Chem.* **1996**, *100*, 16502−16513.
(70) Tao, J.; Perdew, J.; Staroverov, V.; Scuseria, G. Climbing the Density Functional Ladder: Nonempirical Meta-Generalized Gradient Approximation Designed for Molecules and Solids. *Phys. Rev. Lett.* **2003**, *91*, 3−6.
(71) Jalink, J.; Bakker, J. M.; Rasing, T.; Kirilyuk, A. Channeling Vibrational Energy To Probe the Electronic Density of States in Metal Clusters. *J. Phys. Chem. Lett.* **2015**, *6*, 750−754.
(72) Grimme, S.; Antony, J.; Ehrlich, S.; Krieg, H. A Consistent and Accurate Ab Initio Parametrization of Density Functional Dispersion Correction (DFT-D) for the 94 Elements H-Pu. *J. Chem. Phys.* **2010**, *132*, 154104.
(73) Rosi, M.; Bauschlicher, C. W. The Binding Energies of One and Two Water Molecules to the First Transition-Row Metal Positive Ions. *J. Chem. Phys.* **1989**, *90*, 7264.
(74) Jaeqx, S.; Oomens, J.; Cimas, A.; Gaigeot, M. P.; Rijs, A. M. Gas-Phase Peptide Structures Unraveled by Far-IR Spectroscopy: Combining IR-UV Ion-Dip Experiments With Born-Oppenheimer Molecular Dynamics Simulations. *Angew. Chem., Int. Ed.* **2014**, *53*, 3663−3666.

DOI: 10.1021/acs.jpca.5b07119
J. Phys. Chem. A 2015, 119, 10828−10837